

Thermoelectric Properties of a-Site Vacancy La-Sm Co-Doped SrTiO₃ Ceramics

Adindu C. Iyasara* and Felix U. Idu

Department of Ceramic and Glass Technology, School of Industrial Technology, Nigeria

Abstract

Influence of strongly reducing processing atmosphere on Sr-vacancy Sr_{1-3x/2}La_{x/2}Sm_{x/2}TiO_{3-δ} (x=0.05, 0.10, 0.15, 0.20, 0.30) ceramics was investigated. The ceramic powders were prepared by the solid state reaction (SSR) method, and heat treated in 5% H₂/N₂ reducing gas at 1573 K for 6 h and 1773 K for 8 h for calcination and sintering processes, respectively. Thermoelectric properties of Sr_{1-3x/2}La_{x/2}Sm_{x/2}TiO_{3-δ} ceramics were evaluated from 573 K to 973 K. Their electrical conductivities increased with carrier concentration and also decreased with temperature, indicating metallic behaviour. The Seebeck coefficients showed n-type behaviour and increased with temperature. Additionally, the total thermal conductivities exhibited low values, with a minimum value, 2.67 W/m.K for x=0.20 ceramics at 973 K. A maximum thermoelectric figure of merit, ZT=0.30 at 973 K was reached for Sr_{0.7}La_{0.1}Sm_{0.1}TiO_{3-δ} ceramics, which is 20% higher than the maximum value reported previously for La-Sm electron doped SrTiO₃ ceramics.

Keywords: Sr-vacancy • Thermoelectric • Carrier concentration • Thermal conductivity • Figure of merit

Introduction

Thermoelectric (TE) oxide ceramics have been regarded as promising materials for power generation and energy harvesting particularly at high temperatures. Oxides generally are inert, nontoxic, cheap, abundant, thermally stable, resistant to oxidation with a corresponding high temperature, hence potential TE materials for high temperature applications [1,2]. The efficiency of a TE device such as thermoelectric power generator (TEG) depends on the properties of the TE materials which is determined using the dimensionless figure of merit, ZT. This measuring parameter is defined as $ZT = (S^2 \sigma) / k$, where S is a Seebeck coefficient ($\mu\text{V/K}$), σ is an electrical conductivity (S/cm), T is an absolute temperature (K), and k is a thermal conductivity (W/m K²). Therefore, for a high ZT to be achieved, a high power factor, PF ($S^2\sigma$) and a low k are required [3,4].

State of the art TE materials (conventional non-oxides) e.g., PbTe/Se, Bi₂Te₃/Se₃, GeTe, etc. are toxic, scarce, expensive and unstable at high temperatures [5]. Due to their complex structures, they possess low phonon group velocity, leading to low k and optimised ZT values ($ZT \geq 1$) [6-8]. However, a ZT=1 is regarded as a performance benchmark for viable TE materials in the thermoelectrics community [9].

Despite the potential TE characteristics possessed by oxides, they exhibit high k, which leads to low ZT (particularly n-type oxides) when compared to conventional non-oxides. Several n-type oxide materials such as SrTiO₃, ZnO, CaMnO₃ and In₂O₃ have been studied. For example, high ZT values of 0.47 at 1000 K and 0.65 at 1247 K, respectively have been reported for n-type Al-Ga co-doped ZnO and recently $ZT \geq 0.6$ at 1000 K–1100 K for La-Nb co-doped SrTiO₃ [10-12]. Doped and reduced SrTiO₃ ceramics have recently shown improved electrical conductivity required for TE applications [13]. There are various approaches such as doping, co-doping, addition/inclusions, enhanced processing condition, defect and micro/nanostructural engineering so far utilized for optimizing the TE performance of SrTiO₃

[14,15].

In our previous publication a maximum ZT value of 0.24 at 873 K and a minimum k=3.0 W/m [16]. K for x=0.2 at 973 K were obtained for electron La-Sm co-doped SrTiO₃ ceramics. It is therefore established that electron co-doping had a minimal effect on thermal conductivity, hence unsuitable for optimizing ZT. In furtherance to the works reported independently by Kovalevsky et al and Lu et al, it is agreed that batched stoichiometries with cation vacancies followed by processing in reducing atmosphere are milestone in achieving improved thermoelectric properties [14]. This projection informs the aim of this study. It is, therefore, an attempt to improve the TE properties of Sr-site vacancy La-Sm co-doped SrTiO₃ ceramics compared to the previous published electron doped mechanism [16,17].

Experimental

Sr_{1-3x/2}La_{x/2}Sm_{x/2}TiO₃ (x=0.05, 0.1, 0.15, 0.2, 0.3) ceramics were prepared by a solid state reaction (SSR) method. The starting materials of SrCO₃ (99.90%; Sigma-Aldrich, UK), TiO₂ (99.90%; Sigma-Aldrich), La₂O₃ (99.99%; Sigma-Aldrich), and Sm₂O₃ (99.90%; Stanford Materials Corporation, USA) were mixed for 24 h with isopropanol and 10 mm diameter yttria-stabilized zirconia balls using a ball mill. The mixtures were dried at 80°C for several hours and sieved using a 250 μm sieve mesh. The sieved powders were calcined in 5% H₂/N₂ gas at 1573 K for 6 h and then pressed by a uniaxial press into a 20 mm disc pellet (≤ 2 mm thickness). Sintering of the pellets was performed in flowing 5% H₂/N₂ reducing gas at 1773 K for 8 h. Phases of Sr_{1-3x/2}La_{x/2}Sm_{x/2}TiO₃ ceramics were analyzed by x-ray diffraction (XRD) method with a D2 phaser diffractometer (Bruker AXS GmbH, Germany) using Cu K α 1 radiation with $\lambda=1.5406$ Å. Secondary electron (SE) surface images of the ceramics were also observed with a Scanning Electron Microscope (Philips XL 30 S-FEG). Seebeck coefficient and electrical conductivity of the sintered disc pellets were simultaneously measured using a NETZSCH

*Address for Correspondence: Adindu C. Iyasara, Department of Ceramic and Glass Technology, School of Industrial Technology, Nigeria, Email: acnnayrerugo@gmail.com

Copyright: © 2022 Adindu CI, et al. This is an open-access article distributed under the terms of the Creative Commons Attribution License, which permits unrestricted use, distribution, and reproduction in any medium, provided the original author and source are credited.

Received: March 3, 2022; Manuscript No. jme-22-51787 Editor assigned: March 7, 2022; PreQC No: jme-22-51787 Reviewed: March 21, 2022; QC No: jme-22-51787 Revised: March 26, 2022; Manuscript No. jme-22-51787 Published: March 31, 2022; Doi: 10.37421/jme.2022.11.7

SBA 458 NEMESIS instrument in argon atmosphere from 573 K–973 K. The thermal conductivity was determined using a thermal properties analyzer (Anter Flashline TM 3000) while the experimental density was determined by Archimedes' method using an electronic digital density balance (Mettler-Toledo AG Balance).

Results and Discussion

XRD patterns for $\text{Sr}_{1-3x/2}\text{La}_x\text{Sm}_{x/2}\text{TiO}_3$ ($0.05 \leq x \leq 0.3$) ceramics are shown in Figure 1. All samples are single phase and indexed with the SrTiO_3 cubic perovskite structure (pm-3 m space group). The lattice parameters were calculated from the XRD data and the results together with relative densities measured by Archimedes' method are listed in Table 1. The lattice parameters for $x=0.05$ – 0.2 ceramics increase with increasing dopant (La-Sm) concentrations with values ranging from 3.899 to 3.91 Å and decreases for $x=0.3$ (3.902 Å). The increase in lattice parameter is attributed to a decrease in the binding energy within the lattice due to formation of oxygen vacancy and partial reduction of Ti^{4+} ions to Ti^{3+} ions [18]. Structural transitions or distortions and solid solution limit contribute to the decrease in lattice parameter for $x=0.3$ ceramics. However, the lattice parameter trend in this work is contrary to the obtained results in our previously studied electron La-Sm co-doped SrTiO_3 ceramics and in La-Yb co-doped SrTiO_3 [16,19].

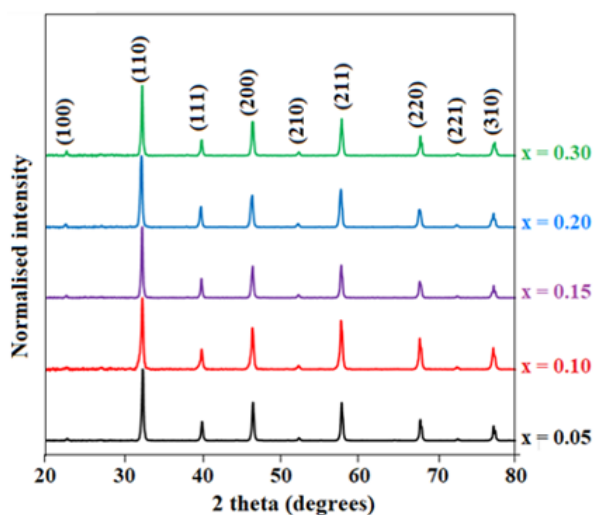


Figure 1. XRD analysis results for $\text{Sr}_{1-3x/2}\text{La}_x\text{Sm}_{x/2}\text{TiO}_3$ ($0.05 \leq x \leq 0.3$) ceramics sintered in 5% H_2/N_2 gas at 1773 K for 8 h

Table 1. List of lattice parameters, cell volumes and relative densities of $\text{Sr}_{1-3x/2}\text{La}_x\text{Sm}_{x/2}\text{TiO}_3$; $0.05 \leq x \leq 0.30$ ceramics sintered in 5% H_2/N_2 gas at 1773K for 8 h.

Composition x	Lattice Parameter (Å)	Cell Volume (Å ³)	Relative Density (%)
0.05	3.899	59.273	98.1
0.1	3.906	59.593	96.1
0.15	3.907	59.639	99.1
0.2	3.91	59.776	98.7
0.3	3.902	59.41	98.2

The relative densities of all ceramics are higher than 96% and higher than most rare earth (RE) doped SrTiO_3 ceramics, [20,21]. The results of microstructure analysis as shown in Figure 2 are identical to the XRD results since no second phases were identified. Therefore, all microstructural images are homogeneous and dense, hence agree with their high relative densities. In addition, these SEM images showed regular polygonal shaped grain structures while the average grain size increased

with increasing doping level. Hence, the average grain size of the ceramics increased from 7.5 μm to 10.4, 10.8 and 11.2 μm for $x=0.10$, 0.15, 0.20 and 0.30, respectively. Comparative analysis shows that these grain sizes are small and evidenced by the adopted highly reducing processing conditions. This assertion is supported by in the literature where a La-Nb co-doped ceramics sintered in air exhibited a larger grain size than the same composition sintered in reducing atmosphere [15]. Reduced grain size implies an incorporation of large grain boundaries which are effective scattering centres for phonons [22].

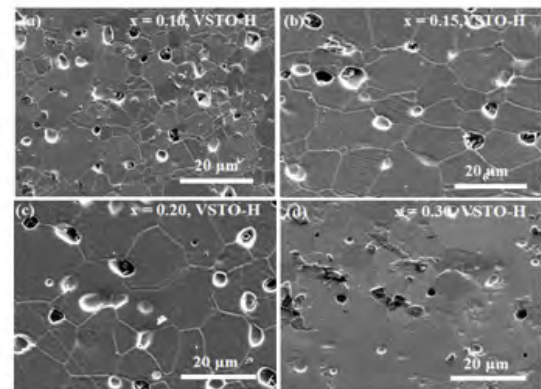


Figure 2. SEM images of the surfaces for $\text{Sr}_{1-3x/2}\text{La}_x\text{Sm}_{x/2}\text{TiO}_3$ ($x = 0.05, 0.15, 0.20, 0.30$) ceramics sintered in 5% H_2/N_2 at 1773 K for 8 h

Temperature dependencies of an electrical conductivity and an absolute Seebeck coefficient for $\text{Sr}_{1-3x/2}\text{La}_x\text{Sm}_{x/2}\text{TiO}_3$ ($0.05 \leq x \leq 0.30$) ceramics are shown in Figure 3. Electrical conductivities for all samples showed a temperature dependence of a degenerate semiconductor or metallic behaviour [23]. As shown in Figure 3a, the electrical conductivity for $x=0.30$ ceramic was higher than all other compositions within the measured temperature range. The reason for the maximum electrical conductivity can be explained by increase of the carrier concentration [9]. High dopant (La^{3+} and Sm^{3+} ions) level substituted into Sr^{2+} sites could contribute to an electrical conductivity of the doped SrTiO_3 ceramics. Consequently, the maximum electrical conductivity of the ceramics was 1023 S/cm at 573K for the $x=0.30$ composition.

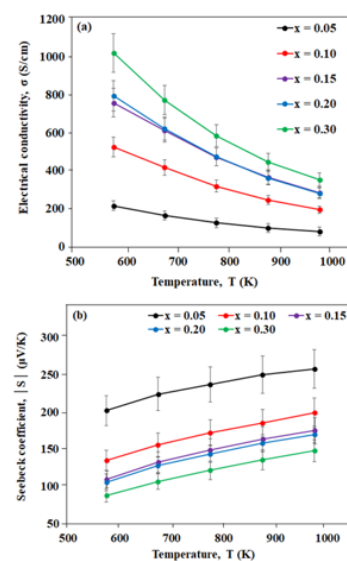


Figure 3. Temperature dependencies of (a) electrical conductivities and (b) absolute Seebeck coefficients for $\text{Sr}_{1-3x/2}\text{La}_x\text{Sm}_{x/2}\text{TiO}_3$ ($0.05 \leq x \leq 0.30$) ceramics sintered in 5% H_2/N_2 at 1773 K for 8 h

Figure 3b shows the absolute Seebeck coefficients for $\text{Sr}_{1-3x/2}\text{La}_x\text{Sm}_{x/2}\text{TiO}_3$

ceramics. Seebeck coefficients of all compositions showed negative for whole temperature range, indicating n-type and increased with temperature, hence an exhibition of metallic behaviour [19]. Generally, a Seebeck coefficient is inversely proportional to a carrier concentration [24]. Accordingly, an increase in carrier concentration (dopant level) for these doped ceramics led to the observed decrease in Seebeck coefficients. However, the average absolute Seebeck coefficients (158–255 $\mu\text{V/K}$) attained in this work at high temperature (973 K) exceeds the minimum recommended Seebeck coefficients (150–250 $\mu\text{V/K}$) for a potential thermoelectric material [25].

Figure 4 represents the temperature dependencies of a total thermal conductivity and a thermoelectric figure of merit for $\text{Sr}_{1-3x/2}\text{La}_{x/2}\text{Sm}_{x/2}\text{TiO}_3$ ceramics. As shown in Figure 4a total thermal conductivity for $x \leq 0.15$ and $x=0.30$ ceramics decreased with increasing temperature up to 873 K and exhibited an abnormal behaviour at high temperature (973 K). The anomaly can be explained by the concept of normal process or scattering (N-process) where momentum is conserved, leading to an increase in thermal conductivity with temperature [26]. $x=0.20$ ceramics showed the lowest total thermal conductivity and decreased with increasing temperature in the whole measurement temperature range. This trend indicates an Umklapp phonon scattering behaviour [12,27]. Overall, a minimum total conductivity, 2.67 W/m. K at 97 K was observed for $x=0.2$ ceramics, comparable to those of doped SrTiO_3 prepared by conventional methods and enhanced techniques [28-31]. The low thermal conductivity obtained indicates an application of reducing atmosphere in all heat treatments (calcination and sintering) has an efficient impact in the thermal properties of SSR synthesized $\text{Sr}_{1-3x/2}\text{La}_{x/2}\text{Sm}_{x/2}\text{TiO}_3$ ceramics.

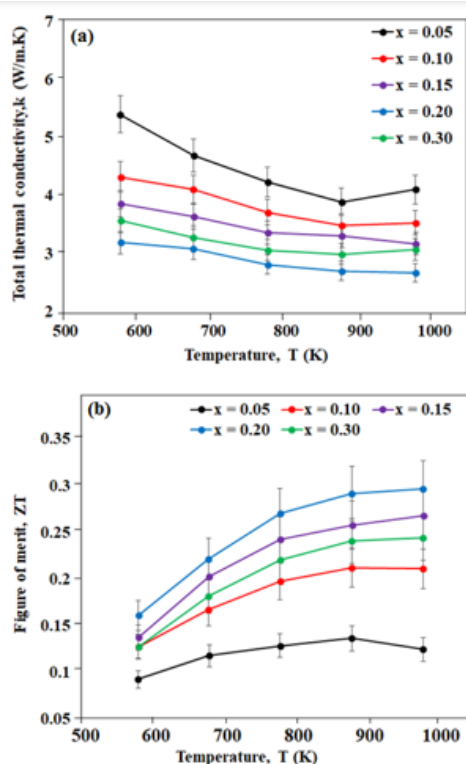


Figure 4. Temperature dependencies of (a) total thermal conductivities and (b) thermoelectric figure of merit for $\text{Sr}_{1-3x/2}\text{La}_{x/2}\text{Sm}_{x/2}\text{TiO}_3$ ($0.05 \leq x \leq 0.30$) ceramics sintered in 5% H_2/N_2 at 1773 K for 8 h

ZT values of ceramics increased with an increase in the dopant level up to $x=0.2$ (Figure 4b) and levels off at $x=0.30$. $x=0.20$ ceramics maintained a leading high ZT over the whole measured temperature range and reached a maximum ZT value of 0.30 at 973 K. This high ZT could be linked to its high lattice parameter and consequent low thermal conductivity.

Conclusion

The influence of strong reducing processing atmosphere and the effect of Sr (cation) vacancy on $\text{Sr}_{1-3x/2}\text{La}_{x/2}\text{Sm}_{x/2}\text{TiO}_3$ ($0.05 \leq x \leq 0.30$) ceramics have been studied. Ceramics were prepared by the reduced SSR method, and their thermoelectric properties were investigated from 573 K–973 K temperature range. The results obtained showed that $\text{Sr}_{1-3x/2}\text{La}_{x/2}\text{Sm}_{x/2}\text{TiO}_3$ ceramics were optimised compared to our previously reported electron doped La-Sm doped SrTiO_3 ($\text{Sr}_{1-x}\text{La}_x/2\text{Sm}_x/2\text{TiO}_3$) ceramics. In $\text{Sr}_{1-x}\text{La}_x/2\text{Sm}_x/2\text{TiO}_3$ ceramics, a highest ZT=0.24 at 873 K for $x=0.15$ was achieved while an optimised ZT value of 0.30 was reported for $\text{Sr}_{1-3x/2}\text{La}_{x/2}\text{Sm}_{x/2}\text{TiO}_3$ ($x=0.20$) ceramics in this work [16]. The minimum total thermal conductivity (2.67 W/m. K) obtained that led to the high ZT was attributed to the creation of Sr-site vacancies and oxygen vacancies resulting from the strongly reducing processing conditions.

Acknowledgments

Financial support from TETFUND Nigeria is greatly acknowledged. I would also like to acknowledge the technical work (experiment)–XRD, SEM and thermoelectric characterization carried out at the functional materials and devices laboratory and the Sorby centre, Department of Materials Science and Engineering, the University of Sheffield, UK.

References

- Iyasara, AC, FU Idu, EO Nwabinele and TC Azubuike, et al. "Thermoelectric study of $\text{La}_2\text{Ti}_2\text{-xNb}_x\text{O}_7$ ($0 \leq x \leq 0.25$) ceramic materials." *J Energy Res Rev* (2020) 6: 38–47
- KH, Jung, SM Choi, CH Lim and HH Park, "Phase analysis and thermoelectric properties of $\text{Zn}_{1-x}\text{M}_x\text{O}$ ($\text{M}=\text{Al}, \text{Ga}$) samples." *Surf. Interface Anal* (2012) 44:1507–1510.
- Tritt, TM and M Subramanian. "Thermoelectric materials, phenomena and applications: A bird's eye view." *MRS Bull* (2006) 31: 188–198
- Nemir, D and J Beck. "On the significance of the thermoelectric figure of merit Z." *J Electron Mater* (2010) 39: 1897–1901
- Jarman, JT, EE Khalil and E Khalaf, "Energy analyses of thermoelectric renewable energy sources." *J Ener Effic* (2013) 2: 143–153
- Kieslich, G. "A chemists view: Metal oxides with adaptive structures for thermoelectric applications." *Phys Stat Soli Appl Mater Sci* (2016) 213: 808–823
- Snyder, GJ and ES Toberer. "Complex thermoelectric materials." *Nat Mater* (2008) 7: 105–114
- Goldsmid, HJ. "Introduction to thermoelectricity." *Sprin Ser Mat Sci* (2010)
- He, J, Y Liu and R Funahashi. "Oxide thermoelectrics: The challenges, progress, and outlook." *J Mater Res* (2011) 26: 1762–1772
- Košir, M, M Podlogar, N Daneu and A Rečnik, et al, "Phase formation, microstructure development and thermoelectric properties of $(\text{ZnO})\text{In}_2\text{O}_3$ ceramics." *J Eur Ceram Soc* (2017) 37: 2833–2842
- Ohtaki, M, K Araki and K Yamamoto, "High thermoelectric performance of dually doped ZnO ceramics." *J Electron Mater* (2009) 38: 1234–1238
- Wang, J, Bo-Yu Z, Hui-Jun K and Yan L, et al. "Record high thermoelectric performance in bulk SrTiO_3 via nano-scale modulation doping." *Nano Energy* (2017) 35: 387–395
- Dawson, JA, X Li, CL Freeman and JH Hardinga, et al. "The application of a new potential model to the rare earth doping of SrTiO_3 and CaTiO_3 ." *J Mater Chem C* (2013) 1: 1574–1582
- Kovalevsky, AV, Myriam HA, Sascha P and Sonia GP, et al. "Designing strontium titanate-based thermoelectrics: Insight into defect chemistry mechanisms." *J Mater Chem A* (2017) 5: 3909–3922
- Srivastava, D, Colin N, Feridoon A and Marion CS, et al. "Tuning the thermoelectric properties of a-site deficient SrTiO_3 ceramics by vacancies and carrier concentration." *Phys Chem Chem Phys* (2016) 18: 26475–26486

16. Iyasara, AC, W Schmidt, R Boston and DC Sinclair, et al. "La and Sm Co-doped SrTiO_{3-x} thermoelectric ceramics." *Mat Tod: Proceed* (2017) 4: 12
17. Lu, Z, H Zhang, W Lei and DC Sinclair, et al. "High figure of merit thermoelectric la-doped a site deficient SrTiO₃ ceramics." *Chem Mater* vol. 28, no. 3, pp. 925–935, 2016
18. Neagu, D and JTS Irvine. "Structure and Properties of La_{0.4}Sr_{0.4}TiO₃ ceramics for use as anode materials in solid oxide fuel cells." *Chem Mater* (2010) 22: 5042–5053
19. Wang, H and C Wang, "Thermoelectric properties of Yb-doped La_{0.1}Sr_{0.9}TiO₃ ceramics at high temperature." *Ceram Int* (2013) 39: 941–946
20. Wang, HC, CL Wang, WB Su and J Liu, et al., "Enhancement of thermoelectric figure of merit by doping Dy in La_{0.1}Sr_{0.9}TiO₃ ceramic." *Mater Res Bull* (2010) 45: 809–812
21. Liu, J, CL Wang, H Peng and WB Su, et al., "Thermoelectric properties of dy-doped SrTiO₃ ceramics." *J Electron Mater* (2012) 41: 3073–3076, 2012
22. Boston, R, WL Schmidt, GD Lewin and AC Iyasara, et al. "Protocols for the fabrication, characterization, and optimization of n-type thermoelectric ceramic oxides." *Chem Mater* (2017) 29: 265–280
23. Wang, HC, CL Wang, Wen BS and Jia L, et al. "Doping effect of La and Dy on the thermoelectric properties of SrTiO₃." *J Am Ceram Soc* (2011) 94: 838–842, 2011
24. Tritt, TM. "Thermoelectric materials: Principles, structure, properties, and applications." *Encycl Mater Sci Technol* (2002): 1–11
25. Dehkordi, AM. "An experimental investigation towards improvement of thermoelectric properties of strontium titanate ceramics." *Clem Univ* (2014)
26. Spiteri, D. "Understanding phonon scattering and predicting thermal conductivity from molecular dynamics simulation." *Univ Bris* (2015)
27. Li, W, S Lin, X Zhang and Z. Chen, et al. "Thermoelectric properties of Cu₂SnSe₄ with Intrinsic vacancy." *Chem Mater* (2016) 28: 6227–6232, 2016
28. Kovalevsky, AV, AA Yaremchenko, S Populoh and P Thiel, et al. "Towards a high thermoelectric performance in rare-earth substituted SrTiO₃: Effects provided by strongly-reducing sintering conditions." *Phys Chem Chem Phys* (2014) 16: 26946–26954
29. Liu, J, CL Wang, Y Li and WB Su, et al. "Influence of rare earth doping on thermoelectric properties of SrTiO₃ ceramics." *J Appl Phys* (2013) 114: 22
30. Ekren, D, F Azough, Ali G and Sarah JD, et al. "Enhancing the thermoelectric power factor of Sr_{0.9}Nd_{0.1}TiO₃ through control of the nanostructure and microstructure." *J Mater Chem A* (2018) 6: 24928–24939
31. Srivastava, D, C Norman, F Azough and MC Schafer, et al. "Improving the thermoelectric properties of SrTiO₃-based ceramics with metallic inclusions." *J Alloys Compd* (2018) 731: 723–730, 2018

How to cite this article: Adindu, CI and Felix U. "Thermoelectric Properties of a-Site Vacancy La-Sm Co-Doped SrTiO₃ Ceramics." *J Material Sci Eng* 11 (2022); 1-4